Journal of Applied Polymer Science

Comparison of initiation methods in the structure of CPAM and sludge flocs properties

Yongjun Sun,[1] Chengyu Zhu,[1] Yanhua Xu,[1] Huaili Zheng,[2] Xuefeng Xiao,[1] Guocheng Zhu,[3] Mengjiao Ren[1]

[1]Jiangsu Key Laboratory of Industrial Water-Conservation & Emission Reduction, College of Environment, Nanjing Tech University, Nanjing 211800, China

[2]Key Laboratory of the Three Gorges Reservoir Region's Eco-Environment, State Ministry of Education, Urban Construction and Environmental Engineering, Chongqing University, Chongqing 400045, China

[3]College of Civil Engineering, Hunan University of Science & Technology, Xiangtan, Hunan 411201, China

Correspondence to: Y. Sun (E-mail: sunyongjun008@163.com)

ABSTRACT: Cationic polyacrylamides (CPAMs) synthesized by thermal, ultrasonic, microwave, and UV initiation were characterized through magnetic resonance hydrogen spectroscopy (^{1}H NMR), Fourier transform infrared spectra, scanning electron microscopy, and thermal gravimetric analysis. The CPAMs for flocculation and dewatering of alum sludge produced through drinking water treatment were evaluated based on the residual turbidity of the supernatant, dry solid content, mean volume diameter and floc size distribution, fractal dimension of the flocs, and zeta potential as a function of flocculant dosage. Comparisons of the characteristics and performance of CPAMs synthesized through different initiation methods were systematically conducted. Flocculation and dewatering test results demonstrated that CPAMs synthesized through microwave and UV initiation had better flocculation performance and dewatering capability than those synthesized through thermal and ultrasonic initiation. All four CPAMs exhibited a similar final floc size distribution but different mean volume diameters and floc structures. The fractal dimension of the flocs and the zeta potential were in the following order: CPAM3 (microwave initiation) > CPAM4 (UV initiation) > CPAM1 (thermal initiation) > CPAM2 (ultrasonic initiation). Discussions on fractal dimension and zeta potential indicated that the electrostatic patches model and adsorption/bridging effect mechanisms played the main role in the formation of sludge flocs. Lastly, microwave and UV initiation were found to be alternative and recommendable initiation methods for the synthesis of CPAMs with improved flocculation performance and sludge dewatering capability. © 2016 Wiley Periodicals, Inc. J. Appl. Polym. Sci. **2016**, *133*, 44071.

KEYWORDS: alum sludge; dewaterability; flocculants; fractal dimension; initiation method

Received 29 March 2016; accepted 6 June 2016
DOI: 10.1002/app.44071

INTRODUCTION

The flocculation–coagulation process is the most common and important process used in sludge pretreatment prior to sludge dewatering. The alum sludge produced in drinking water treatment should be conditioned and dewatered to a certain dry solid (DS) content to meet the recycling requirement or for other final processing procedures.[1] It is a key procedure in the solid–liquid separation process involved in separating waste from sludge as well as in sludge dewatering. Given that the cost of sludge dewatering and its subsequent processing is high and the flocculants employed for sludge flocculation are crucial for sludge–water separation and sludge dewatering,[2] high-performance low-cost flocculants are urgently required in wastewater and sludge dewatering. Organic flocculants as one of the most significant sludge dehydrating agents have elicited much interest.

Organic flocculants play a pivotal role in sludge flocculation and dewatering. Conventional nonionic (anionic) organic flocculants, such as polyacrylamide and anionic polyacrylamide, are widely utilized in sludge conditions, whereas polyacrylamide is suspected to be inefficient in neutralizing negative charges on the surface of fine sludge particles. Many published studies have reported that cationic flocculants with a high molecular weight have good sludge flocculation performance and sludge dewatering capacity.[3,4] The particles experience difficulty flocculating to large flocs for nonionic (anionic) organic flocculants[5] because of the negatively charged fine sludge particles and their small volume. The floc structure is the key parameter that affects sludge properties and dewaterability. Sludge floc properties are mainly determined by the size, size distribution, shape, and fractal dimension of the sludge flocs. Thus, in-depth

© 2016 Wiley Periodicals, Inc.

Table I. Characteristics of CPAMs utilized in the Sludge Conditioning Process

Flocculants	Initiation method	Theoretical CD (%)	Intrinsic viscosity (dL g^{-1})	Dissolving time (h)
CPAM1	Thermal Initiation	30.0	2.12	1.8
CPAM2	Ultrasonic Initiation	30.0	2.12	3.0
CPAM3	Microwave Initiation	30.0	2.11	1.00
CPAM4	UV Initiation	30.0	2.10	1.20

understanding of the structure and properties of sludge flocs is critical to obtain a general comprehension of the sludge flocculation and dewatering mechanism. According to H. Zheng *et al.* and J. Zhu *et al.*,[6,7] the main flocculation mechanism of nonionic (anionic) organic flocculants for negatively charged sludge particles is the absorption and bridge effect. No charge neutralization effect is involved because the flocculants are uncharged or similarly charged. Flocs formed by the absorption and bridge effect are loose, fragile, and easily blocks the filter.[8] However, flocs aggregated by the charge neutralization mechanism are larger and more compact and have better dewatering properties. Sludge flocs have a fractal-like structure and play an important role in flocculation and dewatering.

The formation of floc characteristics is closely related to the type and characteristics of flocculants utilized in the condition process of sludge. Cationic flocculants are thus more effective and efficient in destabilizing negatively charged sludge particles than nonionic (anionic) flocculants. In addition, cationic flocculants are the most commonly used high-cost products in practical engineering applications. The final DS content after dewatering directly depends on the quality and performance of cationic flocculants. Therefore, improved understanding of the interaction mechanisms between cationic flocculants and sludge particles is important for the practical application of cationic flocculants. Currently, many cationic organic polymer flocculants, including cationic polyacrylamides (CPAMs), cationic modified natural organic polymer flocculants, and polydiallyldimethylammonium chloride, are widely utilized in sludge conditioning because of their high-efficiency solid–water separation capability. Specifically, CPAMs elicit much attention because of their high efficiency in improving sludge dewaterability.[9]

CPAMs are usually synthesized through solution polymerization, which is the simplest and most widely used method in industrial processes. However, many initiation methods are available for solution polymerization, including thermal, ultrasonic, microwave, and UV initiation.[10] These four methods are employed in research and practical applications. Many studies have been conducted on one of these four methods. Huaili Zheng *et al.* pointed out that UV-initiated CPAMs have a more porous structure and better flocculation performance than those subjected to thermal initiation.[11] LijuanWang *et al.* demonstrated the superiority of CPAMs initiated by heat over commercial polyacrylamide in the flocculation of kaolin suspension.[12] Sinha Sweta *et al.* studied the microwave-initiated synthesis of flocculants, which exhibited high flocculation efficacy in the treatment of effluents discharged from coal washeries.[13] Chen Wang *et al.* found that ultrasonic-initiated polymerization enhances efficiency without substantially affecting the molecular weight of flocculants.[14] However, comparisons of the characteristics and performance of CPAMs synthesized through different initiation methods have rarely been conducted. Literature has mainly focused on the synthesis of CPAMs by any two of the above-mentioned initiation methods.

This study focuses on the four highly efficient and well-controlled initiation methods for synthesizing CPAMs. CPAMs synthesized by thermal, ultrasonic, microwave, and UV initiation under heterogeneous conditions were characterized through magnetic resonance hydrogen spectroscopy (^{1}H NMR spectra), Fourier transform infrared spectra (FTIR spectra), scanning electron microscopy (SEM), and thermal gravimetric analysis (TG-DSC). Their effectiveness in flocculation performance and sludge dewatering capability were evaluated. The comparative results of the CPAM characterization and the flocculation–sludge dewatering performance were systematically investigated.

EXPERIMENTAL

Materials

The materials employed were acrylamide (AM), 2,2′-azobis(2-methylpropionamide) dihydrochloride (V-50), and 2-(acryloyloxy)ethyl)trimethylammonium chloride (DAC, 80% in water), which were obtained from Aladdin Shanghai Biochemical Technology. All reagents were utilized without further purification. The characteristics of the CPAMs employed in the sludge conditioning process are shown in Table I.

CPAM Synthesis

CPAM was synthesized with AM and DAC. A certain fixed amount of monomers was mixed and dissolved in the reactor under stirring at ambient temperature. The solution was then bubbled with nitrogen gas for 30 min at room temperature to remove oxygen. In the oxygen removal stage, the initiator (V-50) and other additives were added. The initiator (V-50) concentration for all the four initiation methods was 0.5‰ relative to the total monomer concentration. Afterward, the mixed solution was placed in a reactor and initiated through different initiation methods. The thermal initiation reaction was implemented at 40 °C, and the other three initiation reactions (ultrasonic, microwave, and UV) were carried out at room temperature. The lamp use for UV initiation method was a high pressure mercury lamp with 500 W. Its wavelength was 365 nm, and the light intensity was 1800 μw cm^{-2}. The illumination time for UV exposure was 100 min while the microwave reactor was homemade special equipment, it worked for 2 min for

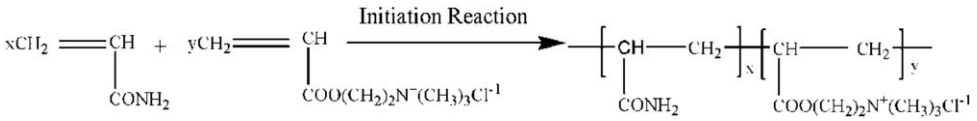

Figure 1. Scheme of the polymerization reaction.

synthesis of CPAM at 800W. The ultrasonic reactors (TENLIN-1000D, Jiang Tenlin Instruments) worked for 30 min at 80 W to synthesize CPAM. After polymerization, the product was purified with acetone and ethanol and then dried in a vacuum oven at 40 °C for subsequent use. The scheme of the reaction route for the preparation of CPAM is shown in Figure 1.

Characterizations of CPAMs

The ^{1}H-NMR spectra of the CPAMs were recorded by an AVANCE 500 NMR spectrometer (BRUKER Company, Germany) with deuterium oxide (D_2O) as the solvent. FTIR spectra were obtained by using a 550Series II infrared spectrometer (BRUKER Company, Switzerland) through the potassium bromide disc technique. SEM of the CPAMs was conducted with a VEGA II LMU SEM system (TES-CAN Company, Czech Republic). Thermal gravimetric analysis (TG-DTA) analysis was conducted with a DTG-60H synchronal thermal analyzer (Shimadzu, Japan) at a heating rate of 10 °C min^{-1} under nitrogen conditions. The intrinsic viscosity of the CPAMs was measured with an Ubbelohde viscometer at 30 °C ± 0.2 °C. The cationic degree (CD) of CPAMs were calculated according to the National Standard of the People's Republic of China, which name was "Water Treatment Chemicals-Technical Specification and Test Method of CPAMs" (GB/T 31246-2014).

Flocculation and Dewatering Experiments

The flocculation performance and sludge dewatering capacity of CPAMs initiated through different methods were evaluated with alum sludge from water treatment plant sludge (a water treatment plant in Chongqing City, China). The dosages of all CPAMs were calculated by their dry weight. The characteristics of sludge from the water treatment plant are shown in Table II. The selected CPAMs synthesized through different initiation methods had the same CD of 30% and the same intrinsic viscosity of 2.1 dL g^{-1}. After rapid stirring at 200 rpm for 2 min and sedimentation for 10 min, the supernatant was immediately extracted for turbidity measurements (HACH 2100Q, US) and zeta potential determination (Zetasizer Nano ZS90, Malvern, UK). Thereafter, the flocculated alum sludge flocs were carefully gathered for the taking of microscope photos of flocs (MIT300 metallurgic microscope, Chongqing OTT Optical Instrument, China), DS content measurement, and sludge floc size distribution determination (BT-9300H laser particle size distribution instrument, Dandong Baite Technology, China). Image-pro Plus 5.0 was utilized to determine the fractal dimensions based on the microscope photographs of alum sludge flocs.

Table II. Characteristics of Sludge from the Water Treatment Plant

pH	Mass density (g mL^{-1})	DS content (%)	Zeta potential (mv)	Al content (mg mL^{-1})
7.0 ± 0.1	1.215	8.52	−8.94	224 ± 10

CPAMs were used to reduce the compressibility of sludge and improve the mechanical strength and permeability of the sludge solid during compression. The cake solids content or filter cake moisture content was often chosen as an index for evaluating the dewaterability of the sludge in full-scale plants.[6,11] The detailed measurement of DS can been seen in a previous study.[15,16] DS content was calculated with the Baerman funnel method using the equation

$$\mathrm{DS} = \frac{W_2}{W_1} \times 100\%,$$

where W_1 is the weight of the wet filter cake after filtration and W_2 is the weight of the filter cake after drying at 105 °C for 24 h.

Fractal dimension was utilized to investigate the nature of flocculants and the flocs. Fractal dimension was calculated using the image analysis method; it is the degree of the linear correlation of the logarithm of the perimeter (L) and area (A). The relationship between projected area and projection perimeter is given by the following formula:[17]

$$\mathrm{A} \sim L^D$$

where A is the projected area (μm^2); L is the projection perimeter (μm); and D is the fractal dimension in 2D space. Performing the natural logarithm in eq. (3), the following form is obtained:

$$\mathrm{Ln}(A) = D\mathrm{Ln}(L) + \mathrm{Ln}(\alpha)$$

where Ln(A) is a dependent variable and Ln(L) is an independent variable. Plotting Ln(A) against Ln(L) yields a straight line with slope D; and Ln(α) is the Ln(A) intercept. These parameters were measured using the software Image-Pro Plus and a microscope.

RESULTS AND DISCUSSION

Characterization of P(AM-DAC-BA)

^{1}H NMR Spectra. The ^{1}H NMR spectroscopies of CPAMs subjected to thermal, ultrasonic, microwave, and UV initiation are shown in Figure 2(a–d), respectively. As shown in Figure 2(a), CPAM was synthesized through UV initiation. The protons of methine and methylene groups in the polymer backbone (—CH_2—CH— in AM and DAC) appeared at 2.12 and 1.53 ppm. The signal that emerged at δ = 4.47 ppm is attributed to the protons in the methylene groups of —O—CH2— (c) in DAC. The protons of methylene groups in —CH_2-N^+ (d) materialized at 3.65 ppm. The most significant signal at δ = 3.12 ppm represents the protons in the three equivalent methyl groups of $N^+(CH_3)_3$ (e) in quaternary ammonium salt. The proton signals of D_2O were observed at δ = 4.70 ppm. As

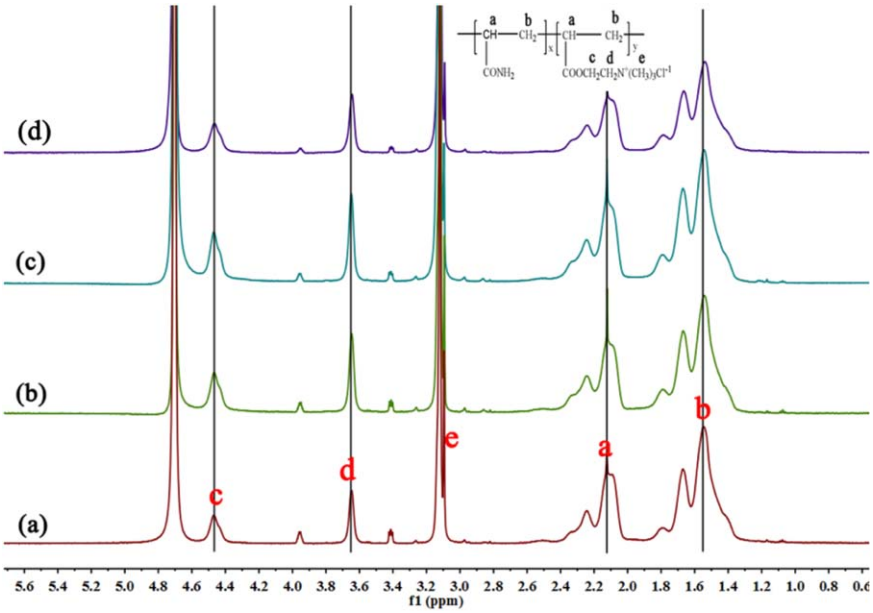

Figure 2. ^{1}H NMR spectra of CPAMs: (a) CPAM1 (thermal initiation), (b) CPAM2 (ultrasonic initiation), (c) CPAM3 (microwave initiation), and (d) CPAM4 (UV initiation). [Color figure can be viewed in the online issue, which is available at wileyonlinelibrary.com.]

reported by the previous studies, the most probable mechanism for the UV-initiated polymerization technology was photo-initiated free-radical polymerization. The dependences of UV-initiated polymerization rate on time, photo-initiator concentration and light intensity shown that classical free-radical polymerization kinetics provided an acceptable quantitative description for UV-initiated polymerization technology.[12,18,19] Compared with Figure 2(b–d), the ^{1}H NMR spectroscopies of CPAM subjected to thermal, ultrasonic, microwave, and UV initiation were similar but exhibited a slight change in chemical shift.[20] Figure 2 also shows that the different initiation methods had almost no effect on the ^{1}H NMR spectroscopies of CPAM. ^{1}H NMR spectroscopy confirmed that the polymers of AM and DAC have been successfully synthesized through thermal, ultrasonic, microwave, and UV initiation.

FTIR Spectra

Figure 3 shows the FTIR spectra of CPAMs subjected to thermal, ultrasonic, microwave, and UV initiation. In the FTIR spectrum of the CPAM initiated through UV initiation, the band at 3312.7 cm^{-1} is ascribed to the stretching vibration absorption peak of the amino group (—NH_2). A strong water absorption peak was observed at 3173.3 cm^{-1} because the CPAM had high water solubility and strong water-absorbing capacity. The asymmetric absorption peak at 2928.6 is attributed to the characteristic peak of methyl and methylene. The absorption peaks at 1729.2 and 1405.3 cm^{-1} are attributed to the stretching vibration absorption peak of C═O and the bending vibration absorption peak of C—O—C in the ester group (—$COOCH_2$—), respectively. The band at 1648.1 cm^{-1} is assigned to the characteristic absorption peak of the acyloxy group. The characteristic absorption peak at 1405.3 cm^{-1} is ascribed to the bending vibration–absorption peak of —CH_3 in the —CH_2—$N^{+}(CH_3)_3$ group in DAC. The band at 947.2 cm^{-1} is assigned to the characteristic absorption peak of quaternary ammonium salt, which is the characteristic absorption peak of DAC. All these bands are common in the spectra of AM, DAC, and their copolymer because of the presence of the AM and DAC monomer.[21] Infrared spectroscopy showed that the resulting product is a copolymer of AM and DAC. Comparing Figure 2(d) with Figure 2(a–c), the spectrum structures are similar but exhibit a slight shift in wavenumber and peak intensity. These FTIR characterization results demonstrate that the copolymer of AM and DAC was successfully obtained by all four initiation methods. The initiation method had minimal influence on the FTIR spectroscopy of CPAMs.

SEM Result

Figure 4(a–d) show the SEM images of CPAMs synthesized by thermal, ultrasonic, microwave, and UV initiation, respectively. As shown in the Figures, the initiation method had essential

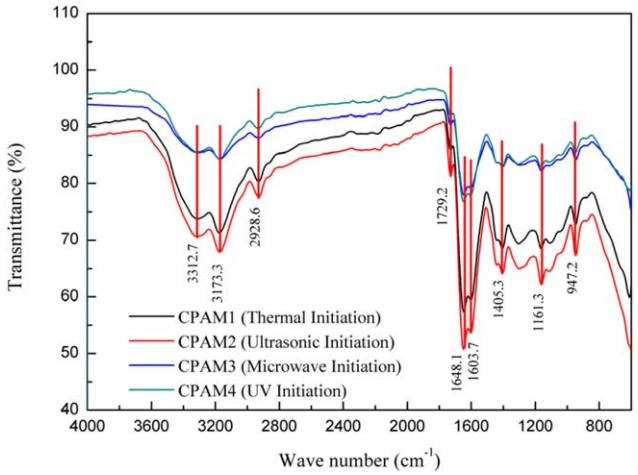

Figure 3. FTIR spectra of CPAMs. [Color figure can be viewed in the online issue, which is available at wileyonlinelibrary.com.]

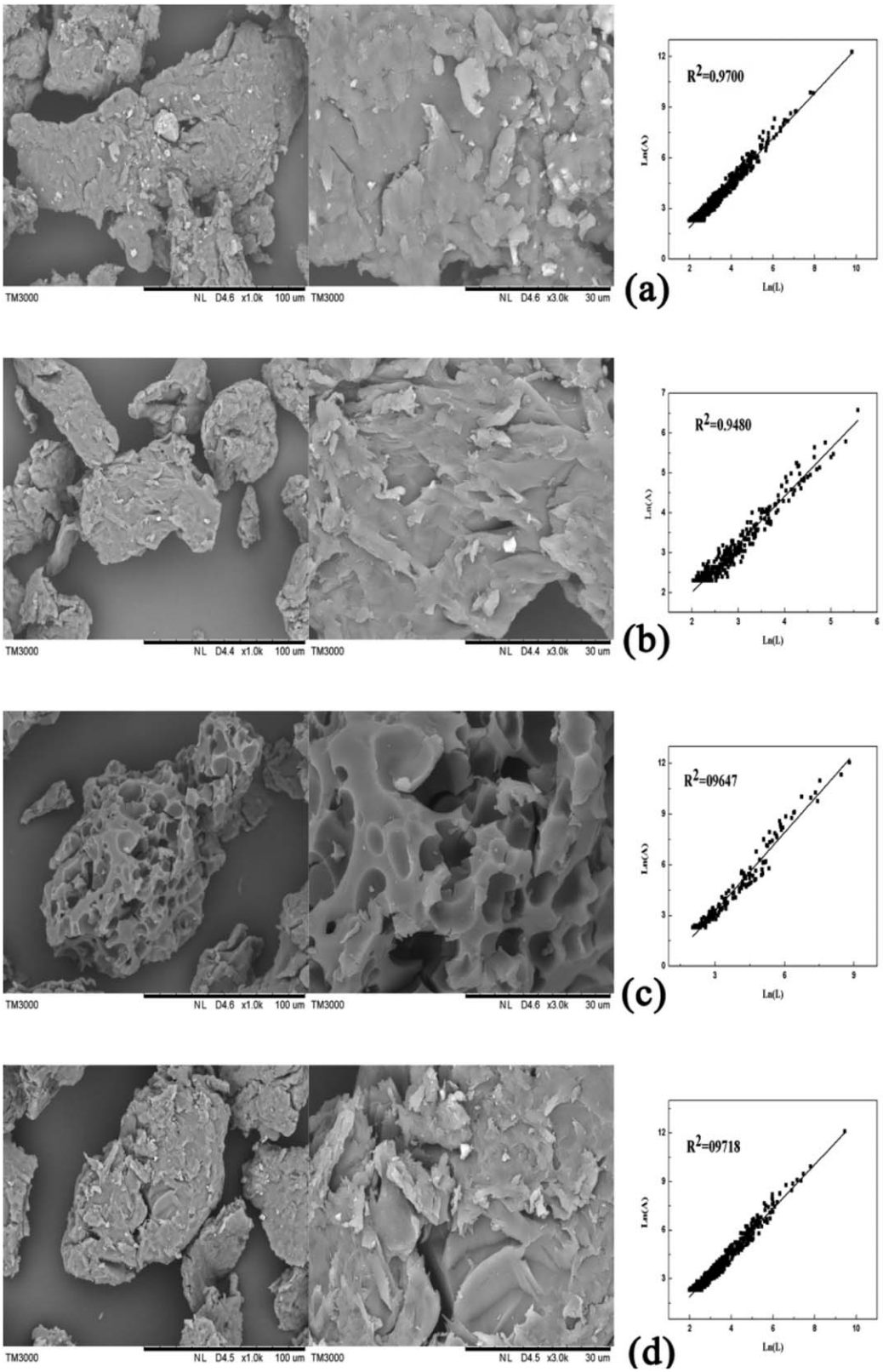

Figure 4. SEM images of CPAMs: (a) CPAM1 (thermal initiation), (b) CPAM2 (ultrasonic initiation), (c) CPAM3 (microwave initiation), and (d) CPAM4 (UV initiation).

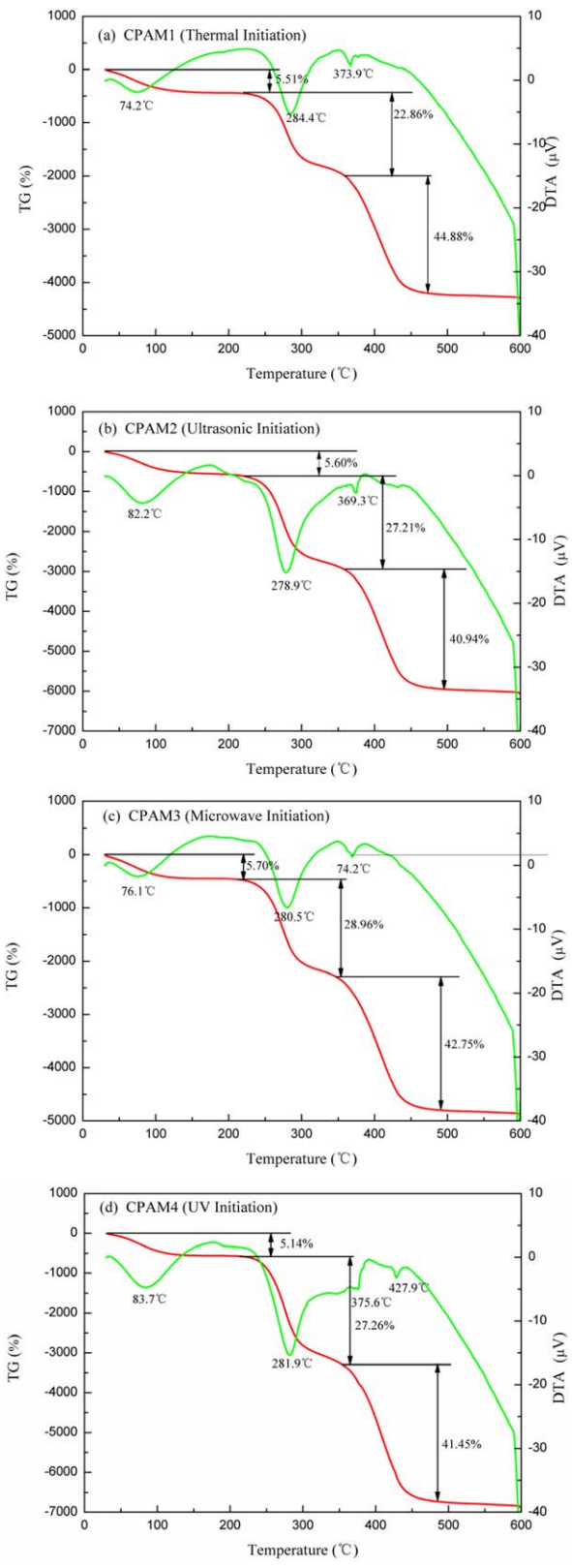

Figure 5. Thermal gravimetric curve of CPAMs: (a) CPAM1 (thermal initiation), (b) CPAM2 (ultrasonic initiation), (c) CPAM3 (microwave initiation), and (d) CPAM4 (UV initiation). [Color figure can be viewed in the online issue, which is available at wileyonlinelibrary.com.]

significant effect on the surface morphology of CPAM. Surface morphology with large bulges, such as ellipticals, was observed in the SEM image of CPAMs subjected to thermal initiation. Figure 4(b) shows a large number of banded bulge structures. However, the main difference was the numerous macroporous structures with a pore size between 5 and 15 μm observed in Figure 4(c). Literature indicates that a porous structure is conducive for the improvement of the solubility of flocculants.[6] Many fibrous and lamellar structures were observed on the surface image of CPAM synthesized by UV initiation. The significant and most obvious difference in the surface morphology of the CPAMs synthesized by the different initiation methods was the different generation mechanism of free radicals. Different means of initiation resulted in different generation modes of free radicals, which in turn resulted in a discrepant intensity of the polymerization reaction and different surface morphologies of the polymers.

Fractal dimension was utilized to investigate the nature of flocculants. Fractal dimension was calculated using the image analysis method; it is the degree of the linear correlation of the logarithm of the perimeter (L) and area (A).[22] According to the result of fractal dimension calculated with the Image-Pro Plus 6.0 software, the average fractal dimensions of CPAMs synthesized by thermal, ultrasonic, microwave, and UV initiation were 1.324, 1.205, 1.552, and 1.358, respectively. The fractal dimension of the CPAM subjected to microwave initiation was higher than the fractal dimensions of the three other CPAMs; the fractal dimension of the CPAM subjected to ultrasonic initiation was the lowest. The differences in fractal dimension were caused by different surface morphologies. This result indicates that the products synthesized by the different initiation methods had different physical and chemical properties. However, the CPAM synthesized by microwave initiation had a more porous structure compared with the CPAMs synthesized by the other three initiation methods.[23] Akkaya *et al.* pointed out that flocculants with porous structures have better solubility and flocculation performance.[24] In contrast to this discussion, the effect of microwave initiation contributed to the formation of a porous structure, thereby helping increase the solubility of flocculants.

TG-DTA Analysis

Figure 5 shows the TG-DTA curve of the CPAMs initiated through the four initiation methods. Figure 5(a) shows the TG curve of the CPAM subjected to thermal initiation. As shown in Figure 5(a), the first-stage weight loss temperature range was 30–230 °C, and the weight loss within this range was 5.51%; this result is due to the removal of adsorbed water. The polymerization products were polyacrylamide flocculants with excellent solubility used in water treatment and a large number of hydrophilic groups resulting in strong moisture absorption of the dry sample. The second-stage weight loss temperature range was 230–360 °C, and the weight loss within this range is 22.86%. The sample weight loss may be due to the thermal decomposition of amide groups (—CO—NH—) with dehydrogenation and demethylation of quaternary ammonium groups on ($—C(CH_3)_3N^+$ Cl^-). The third-stage weight loss temperature range was 360–470 °C; the polymer main chain began to

Table III. Thermal Gravimetric Parameter by the Four Initiation Methods

		Initiation method			
	Parameter	Thermal initiation	Ultrasonic initiation	Microwave initiation	UV initiation
First stage	Temperature range (°C)	30–230	30–220	30–220	30–220
	Weight loss (%)	5.51	5.60	5.70	5.14
	Maximum weight loss temperature (°C)	74.2	82.2	76.1	83.7
Second stage	Temperature range (°C)	230–360	220–360	220–355	220–365
	Maximum weight loss temperature (°C)	284.4	278.9	280.5	281.9
	Weight loss (%)	22.86	27.21	28.96	27.26
Third stage	Temperature range (°C)	360–470	360–490	355–490	365–490
	Maximum weight loss temperature (°C)	373.9	369.3	374.2	375.6/427.9
	Third stage weight loss (%)	44.88	40.94	42.75	41.45
Fourth stage	Temperature range (°C)	470–600	490–600	490–600	490–600
	Residual weight (%)	26.75	26.25	22.59	26.15
	T_g (°C)	230	275	170	175

decompose through an endothermic degradation reaction. The vast weight loss was 44.88%, and ultimately, the complete decomposition temperature was ~470 °C.[25] After 470 °C, the TG curve flattened, with no weight loss produced. The final residual weight was 26.75%.

As shown by the DTA curve in Figure 5, the endothermic peak in the range of 30–230 °C corresponds to the first phase of weight loss, which is due to the endothermic gasification of absorbed moisture in the dry polymer sample. The endothermic peak in the range of 230–360 °C corresponds to the second stage of weight loss, which may be due to the thermal decomposition reaction of the amide group. The last endothermic peak within the range of 360–470 °C corresponds to the third stage of weight loss, which is due to the degradation of the polymer. The glass transition temperature (T_g) of the CPAM synthesized by thermal initiation was 206.33 °C, and the decomposition temperature was 284.4 °C. The TG-DTA curves showed that the polymer was the copolymer of AM and DAC rather than a combination of two homopolymers.[26,27] CPAM was stable when it was used in the wastewater and sludge treatment process at room temperature. A summary of the TG parameter by the four initiation methods is shown in Table III.

In Figure 5(a–d), the TG-DTA curves demonstrate that the CPAMs were successfully synthesized by the four initiation methods. Table III shows that the thermal properties are similar, including the weight loss temperature range, weight loss at each stage, and maximum weight loss temperature. However, the T_g of the CPAMs synthesized by thermal and ultrasonic initiation was significantly higher than that synthesized by microwave and UV initiation. Table III also demonstrates that the CPAMs synthesized by thermal and ultrasonic initiation have better thermal stability.

Comparison of the Initiation Methods' Sludge Dewatering Performance

Effect of Dosage on Dewatering Performance. Figures 6 and 7 show the effect of flocculant dosage on sludge dewatering performance. With the increase in dosage, the residual turbidity of the supernatant generally increased after flocculation. However, the residual turbidity of the supernatant flocculated by CPAM1, CPAM2, and CPAM3 decreased slightly at 10 mg L^{-1}, and the minimum residual turbidity flocculated by CPAM1 and CPAM4 at 10 mg L^{-1} were 18.7 and 14.1 NTU, respectively. This result is due to the waterworks test implemented with PAC as a coagulant; strong electrostatic repulsions occurred between cationic flocculants and positively charged poly aluminum chloride (PAC) in the waterworks sludge. The electrostatic repulsion

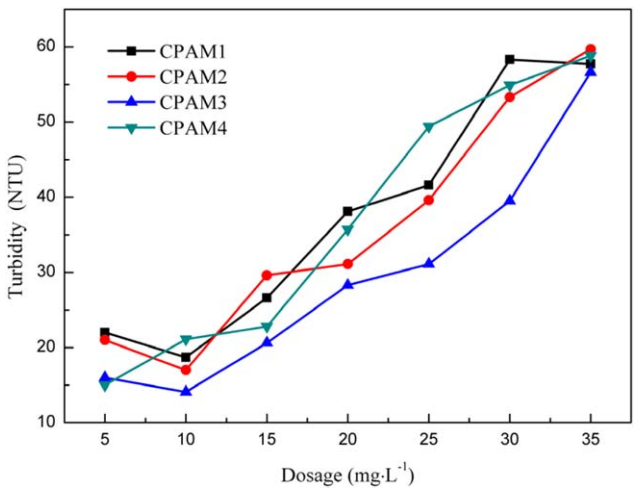

Figure 6. Effect of dosage on the residual turbidity of the supernatant. [Color figure can be viewed in the online issue, which is available at wileyonlinelibrary.com.]

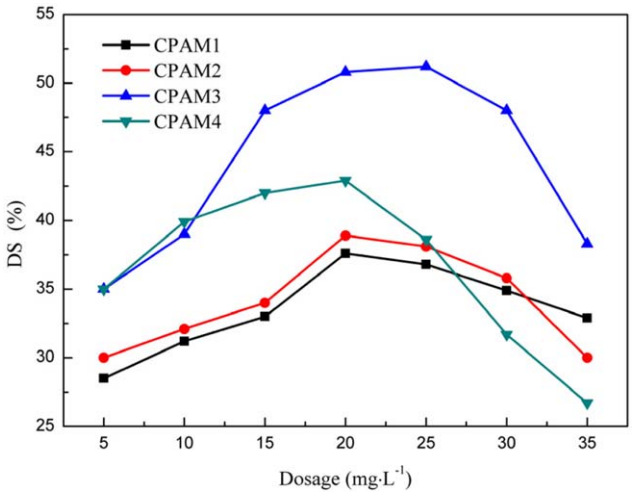

Figure 7. Effect of dosage on DS. [Color figure can be viewed in the online issue, which is available at wileyonlinelibrary.com.]

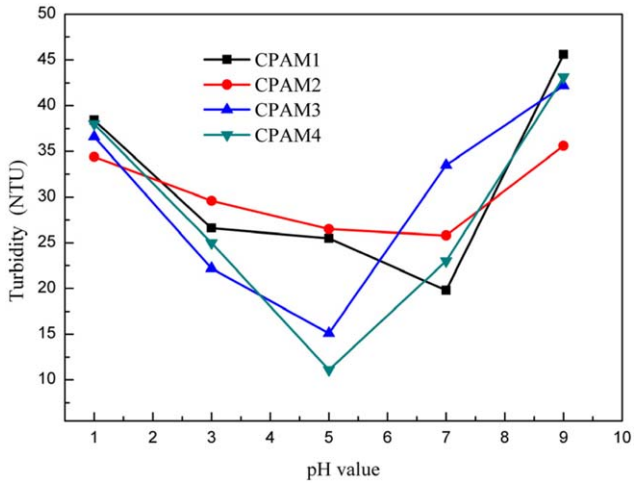

Figure 8. Effect of pH on the residual turbidity of the supernatant. [Color figure can be viewed in the online issue, which is available at wileyonlinelibrary.com.]

between PAC and organic flocculants led to the escape of fine particles from the flocs, which in turn resulted in suspended particle concentration and increase in supernatant turbidity.[28]

The residual turbidity of the supernatant continued to increase with the increase in flocculant dosage. However, Figure 6 shows that the supernatant residual turbidity flocculated by CPAM3 was significantly lower than that flocculated by CPAM1, CPAM2, and CPAm4. This finding indicates that CPAM3 had better electrical neutralization ability and adsorption bridging performance than the other three CPAMs.[29,30]

Figure 7 demonstrates that with the increase in dosage, the solid content after sludge dewatering initially increased and then decreased sharply. The maximum solid contents flocculated by CPAM1, CPAM2, CPAM3, and CPAM4 at 20, 20, 25, and 20 mg L^{-1} were 37.6, 38.9, 51.2, and 42.9%, respectively. When the dosage was in the range of 10–25 mg L^{-1}, the solid content of each flocculant synthesized by the different initiation methods was in the following order: CPAM3 > CPAM4 > CPAM2> CPAM1. The solid contents flocculated by CPAM3 and CPAM4 after sludge dewatering were significantly higher than those flocculated by CPAM1 and CPAM2, further demonstrating that the CPAMs synthesized by microwave and UV initiation had a stronger electric neutralization capability to efficiently neutralize negative charges on the sludge particle surface. A much longer and linear chain strengthened the adsorption bridging role in the sludge flocculation process. In conclusion, the optimal sludge flocculation dosage range is 10–30 mg L^{-1}

Effect of pH on Dewatering Performance

The pH value played a vital role in the flocculation process by changing the chemical forms of the flocculating object and flocculates. The effect of pH values on the residual turbidity of the supernatant is shown in Figure 8. With the increase in pH value, the supernatant turbidity also increased; the pH value showed an increasing trend after the initial decrease. The minimum supernatant turbidity flocculated by CPAM3 and CPAM4 was obtained at pH 5, whereas the minimum supernatant turbidity flocculated by CPAM1 and CPAM2 was obtained at pH 7. The minimum residual turbidity of the supernatant of CPAM1, CPAM2, CPAM3, and CPAM4 was 19.8, 25.8, 15.1, and 11.1 NTU, respectively. The residual supernatant turbidity of CPAM3 and CPAM4 was lower than that of CPAM1 and CPAM2 at pH 5. The residual turbidity of the supernatant at pH 11 was considerably greater than that at other pH conditions, and the residual turbidity of the supernatant of CPAM1, CPAM2, CPAM3, and CPAM4 was 168, 845, 954, and 762 NTU, respectively.

Figure 9 shows the effect of pH value on DS content. With the increase in pH value, the DS content of dewatered sludge initially increased and then decreased drastically. The maximum DS content was obtained at pH 7. The maximum DS content of CPAM1, CPAM2, CPAM3, and CPAM4 was 37.6, 38.9, 51.8, and 48%, respectively. Comparison of the DS content at various pH values indicated that the CPAMs synthesized by microwave and UV initiation had better sludge flocculation performance than those synthesized by thermal and ultrasonic initiation.

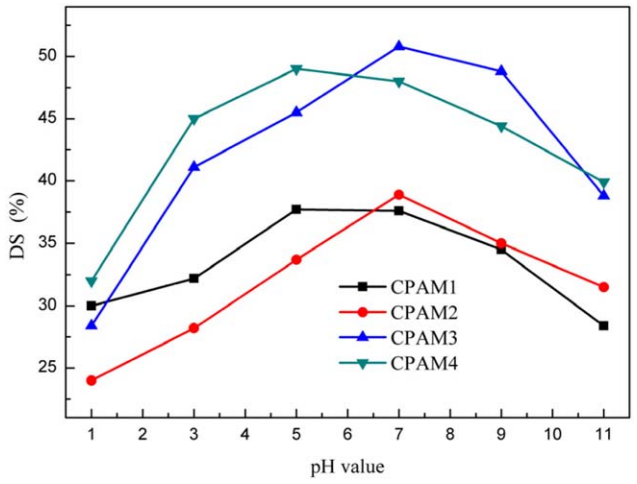

Figure 9. Effect of pH on DS. [Color figure can be viewed in the online issue, which is available at wileyonlinelibrary.com.]

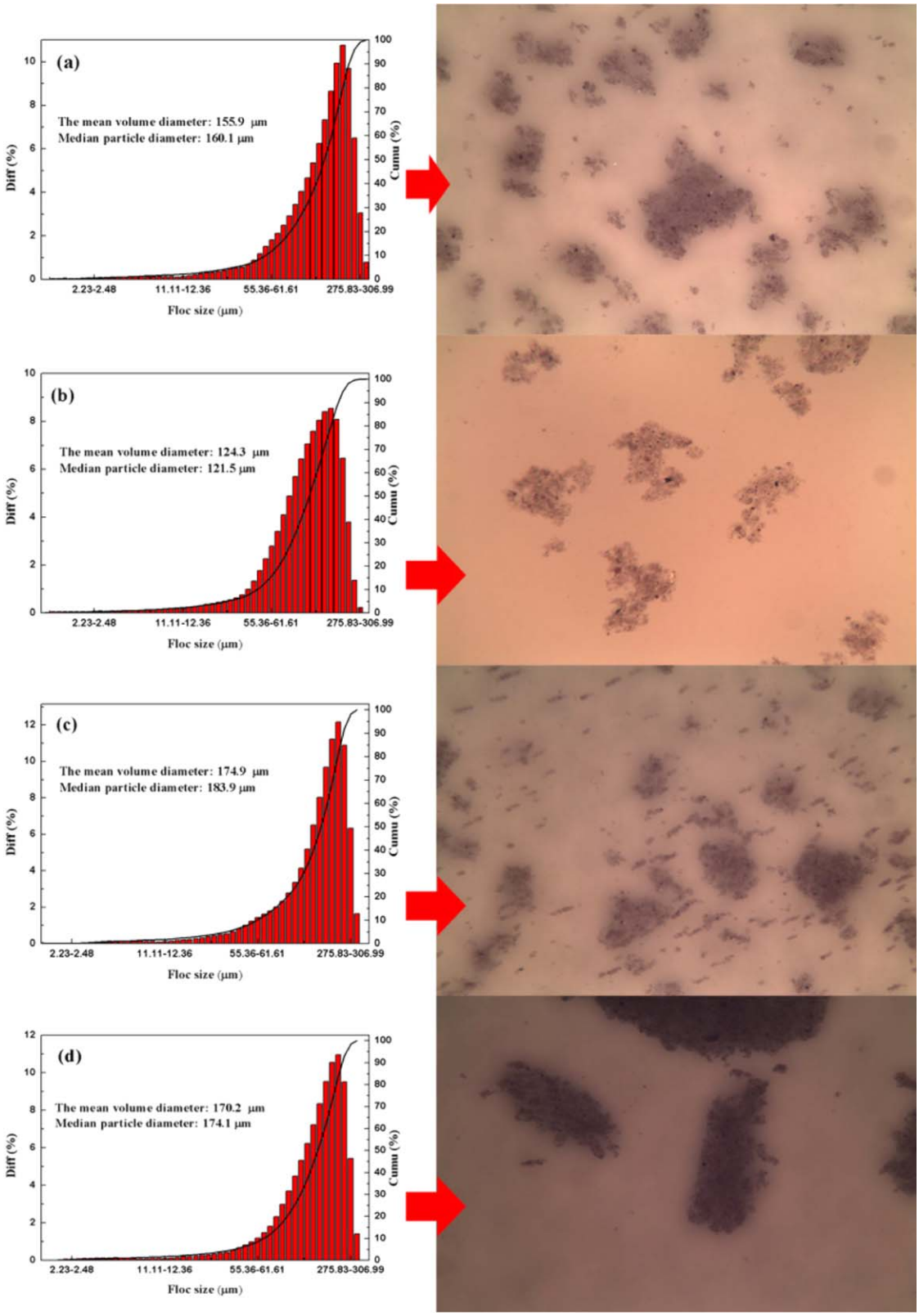

Figure 10. Effect of initiation method on floc size distribution: (a) CPAM1 (thermal initiation), (b) CPAM2 (ultrasonic initiation), (c) CPAM3 (microwave initiation), and (d) CPAM4 (UV initiation). [Color figure can be viewed in the online issue, which is available at wileyonlinelibrary.com.]

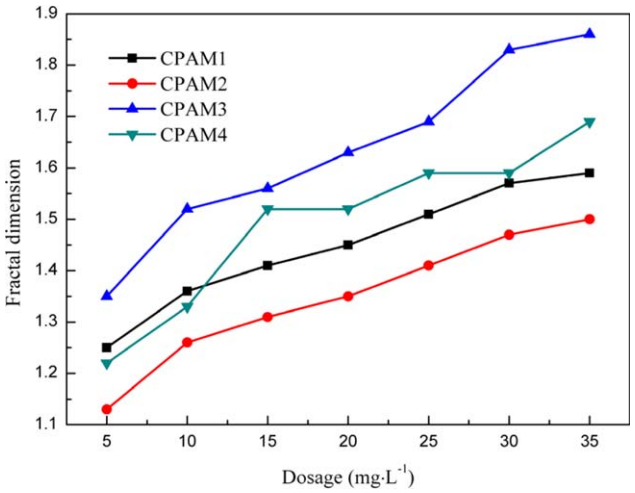

Figure 11. Effect of dosage on fractal dimension. [Color figure can be viewed in the online issue, which is available at wileyonlinelibrary.com.]

Sludge dewatering performance at pH 5–9 was better than that under strong acidic or strong alkaline conditions. In summary, a relatively broad pH range of 5–9 is the optimal pH range for sludge dewatering.

A possible explanation for the poor sludge dewatering performance under strongly acidic conditions is that PAC in the sludge coagulants was changed into Al^{3+}, and dissolved Al^{3+} eluted from the sludge made the supernatant full of fine sludge particles, thereby increasing the residual turbidity of the supernatant and reducing the sludge dewatering performance. In the strongly alkaline condition, the supernatant was turbid and yellow. This phenomenon may be due to the hydrolysis of PAC into a large number of evenly distributed and stable aluminum hydroxide particles suspended in the supernatant. The hydrolysis of PAC made the sludge particles extremely fine that the sludge dewatering performance deteriorated. Thus, the hydrolysis of aluminum coagulants in the sludge particles changed the aluminum species and sludge particle structure under strongly acidic and alkaline conditions, resulting in flocculation performance deterioration. This explanation is consistent with that in previous studies.[31,32] The pH value also affected the stretching degree of organic polymer flocculant chains in the solution and further changed the electric neutralization capability and adsorption bridging role.

Effect of Dosage on Floc Size Distribution

The effect of initiation method on floc size distribution is shown in Figure 10. The mean volume diameter flocculated by the CPAMs synthesized by thermal, ultrasonic, microwave, and UV initiation was 155.9, 124.3, 174.9, and 170.2 μm, respectively. The mean volume diameter flocculated by CPAM3 and CPAM4 was significantly larger than that flocculated by CPAM1 and CPAM2. This result indicates that the CPAMs synthesized by microwave and UV initiation had better sludge flocculation performance and generated larger sludge flocs. The floc size distribution exhibited by CPAM3 and CPAM4 was narrower than that exhibited by CPAM1 and CPAM2. The mean volume diameter of floc size and the floc size distribution are consistent with those in the floc micrographs (illustrated on the right side). Meanwhile, the flocs formed by UV-induced CPAM1 were denser than those formed by CPAMs initiated by the three other methods. Certain fine sludge particles were present between the sludge flocs, as can be seen in the flocs micrograph in Figure 10. This result is due to the small raw sludge particles and floc multilayer structure that formed during the flocculation process, resulting in the escape of fine sludge particles from the sludge flocs. The particle size and particle size distribution of the sludge were the key factors that affected the performance of sludge dewatering. The fine particles were difficult to precipitate because of colloidal stability. Meanwhile, the fine sludge particles easily penetrated the filter and increased the water content of dewatered sludge. The floc aggregates generated by CPAMs initiated by microwave and UV initiation had less fine particles and demonstrated better sludge flocculation performance and sludge dewaterability.[33]

Previous studies have reported that large floc particle sizes are conducive for the improvement of sludge dewatering performance, reduction of sludge specific resistance, and increase of DS content after dewatering.[34–36] The larger the particle size of the sludge after flocculation is, the better the sludge dewatering is. Considering that the sludge particles are gels, small sludge particles had a relatively large specific surface area and surface tension and thus adsorbed a large amount of water. When the particle size increased, the specific surface area, surface tension, and absorbed water decreased, resulting in a change in the sludge floc structure; consequently, sludge dewatering performance was improved. This result is consistent with previous research results (Figures 7–9).

Effect of Dosage on Fractal Dimension and Zeta Potential

Dewatering performance is closely related to the structure of the floc, and fractal dimension is a crucial parameter to provide information on the structure of sludge flocs. A large fractal dimension means dense sludge flocs and good sludge dewaterability. Figure 11 shows the effect of dosage on the fractal dimension. With the increase in dosage, the fractal dimension

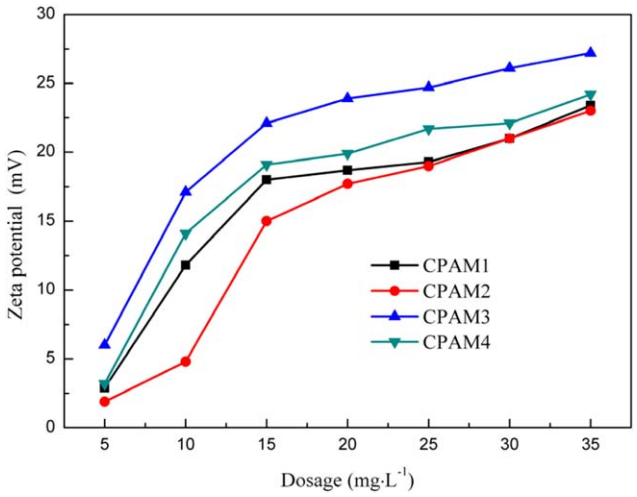

Figure 12. Effect of dosage on Zeta potential. [Color figure can be viewed in the online issue, which is available at wileyonlinelibrary.com.]

increased. When the dosage was more than 10 mg L^{-1}, the fractal dimension was in the following order: CPAM3 (microwave initiation) > CPAM4 (UV initiation) > CPAM1 (thermal initiation) > CPAM2 (ultrasound initiation). According to Figure 10, the sludge flocs with a large fractal dimension always had a large floc size, and the fractal dimension order was basically consistent with the floc size order in Figure 10. The fractal dimension was in the range of 1.10–1.90, which is consistent with that reported in literature using the image method to measure the fractal dimension of sludge flocs.[37]

Figure 12 shows the effect of dosage on the Zeta potential. With the increase in flocculant dosage, the Zeta potential was always positive and continued to increase. The Zeta potential flocculated by the CPAMs synthesized by the different initiation methods was in the following order: CPAM3 (microwave initiation) > CPAM4 (UV initiation) > CPAM1 (thermal initiation) > CPAM2 (ultrasonic initiation). The Zeta potential of microwave-induced CPAM3 was the highest, which indicates that it had the strongest charge neutralization ability. The Zeta potential of raw sludge supernatant was −9.04 mV, but it increased quickly with the dosage of the flocculants. The negatively charged sludge particles with $[Al(OH)^{4-}]$ were rapidly neutralized, and the sludge system transformed from negative to positive. When the dosage of CPAM continued to increase, the sludge system had no negative charge to be neutralized.[38] However, good flocculation performance and high DS content were still obtained mainly because of the absorption and bridge effect of the flocculants' polymer chain.

The electrostatic patches model mechanism is also another possible explanation for the aforementioned phenomenon. The negative charge was non-uniformly distributed on the surface of sludge colloidal particles. The negatively charged areas on the surface of sludge particles could still be neutralized by overdosing CPAM. Therefore, the main mechanism for flocculating the water treatment sludge was the adsorption bridging flocculation effect and electrostatic patches model mechanism.[39]

CONCLUSIONS

A systematic comparison was conducted among CPAMs synthesized by four initiation methods for a better evaluation of their structural characteristics. Moreover, a series of experimental procedures were developed to compare the flocculation behavior and floc structure characteristic of the CPAMs synthesized by the four initiation methods in terms of flocculating and dewatering aluminum-coagulated water treatment residuals. The following conclusions were obtained from the results.

FTIR and ^{1}HNMR provided evidence that the copolymers were successfully synthesized. The SEM results showed that the CPAM synthesized by microwave initiation had a more porous structure than those synthesized by the three other initiation methods. TG-DTA analysis demonstrated that the copolymer had favorable thermal stability in the wastewater and sludge treatment without degradation. In addition, the CPAMs synthesized by thermal and ultrasonic initiation had good thermal stability.

The flocculation and sludge dewatering results showed that the optimum dosage range of CPAM1 (thermal initiation), CPAM2 (ultrasonic initiation), CPAM3 (microwave initiation), and CPAM4 (UV initiation) was 15–30 mg L^{-1}. The applicable pH range was between 5 and 9, and the highest DS content of 51.8% was obtained at pH 7 and 20 mg L^{-1}. At the optimal flocculant dosage, the flocculation rate and DS content of CPAM3 and CPAM4 were remarkably larger than those of CPAM1 and CPAM2, indicating that microwave and UV initiation were beneficial to the improvement of the flocculation performance and sludge dewatering ability of CPAM.

The mean volume diameters of flocs formed by CPAM3 and CPAM4 were significantly larger than those formed by CPAM1 and CPAM2. Moreover, the flocs formed by CPAM3 and CPAM4 presented a better flocculation and sludge dewatering capacity based on the narrow floc size distribution than the flocs formed by CPAM1 and CPAM2. The discussion on the Zeta potential revealed that the flocs were formed by the charge neutralization mechanism and absorption and bridge effect and might be held together by the electrostatic patches model mechanism.

In conclusion, the findings suggest that CPAMs are applicable and can be efficiently utilized for the flocculation of water treatment sludge prior to sludge dewatering. Microwave and UV initiation are effective methods of synthesizing CPAM with high flocculation performance and sludge dewaterability.

ACKNOWLEDGMENTS

This research was supported by the National Natural Science Foundation of China (No. 51508268, No. 51408215), the Natural Science Foundation of the Jiangsu Province in China (No. BK20150951), and China Postdoctoral Science Foundation (No. 2016M591835).

REFERENCES

1. Wang, J. P.; Chen, Y. Z.; Ge, X. W.; Yu, H. Q. *Chemosphere* **2007**, *66*, 1752.
2. Feng, G.; Liu, L.; Tan, W. *Ind. Eng. Chem. Res.* **2014**, *53*, 11185.
3. Guo, J.; Nengzi, L.; Zhao, J.; Zhang, Y. *Appl. Microbiol. Biotechnol.* **2015**, *99*, 2989.
4. Lu, L.; Pan, Z.; Hao, N.; Peng, W. *Water Res.* **2014**, *57*, 304.
5. Verrelli, D. I.; Dixon, D. R.; Scales, P. *J. Water Res.* **2010**, *44*, 1542.
6. Zheng, H.; Sun, Y.; Guo, J.; Li, F.; Fan, W.; Liao, Y.; Guan, Q. *Ind. Eng. Chem. Res.* **2014**, *53*, 2572.
7. Zhu, J.; Zhang, G.; Li, J. *J. Appl. Polym. Sci.* **2011**, *120*, 518.
8. Ariffin, A.; Razali, M. A. A.; Ahmad, Z. *Chem. Eng. J.* **2012**, *179*, 107.
9. Wei, J.; Gao, B.; Yue, Q.; Wang, Y.; Li, W.; Zhu, X. *Water Res.* **2009**, *43*, 724.
10. Casimiro, M. H.; Botelho, M. L.; Leal, J. P.; Gil, M. H. *Phys. Chem.* **2005**, *72*, 731.

11. Zheng, H.; Sun, Y.; Zhu, C.; Guo, J.; Zhao, C.; Liao, Y.; Guan, Q. *Chem. Eng. J.* **2013**, *234*, 318.
12. Wang, L.; Wang, J.; Zhang, S.; Chen, Y.; Yuan, S.; Sheng, G.; Yu, H. *Sep. Purif. Technol.* **2009**, *67*, 331.
13. Sweta, S.; Sumit, M.; Gautam, S. *Int. J. Biol. Macromol.* **2013**, *60*, 141.
14. Wang, C.; Li, X.; Shen, Y.; Li, P. *J. Polym. Res.* **2013**, *20*, 50.
15. Wu, B.; Chai, X.; Zhao, Y. *Bioproc. Biosyst. Eng.* **2016**, *4*, 627.
16. (a) Liu, J.; Yang, Q.; Wang, D.; Li, X.; Zhong, Y.; Li, X.; Deng, Y.; Wang, L.; Yi, K.; Zeng, G. *Bioresour. Technol.* **2016**, *206*, 134. (b) Sun, Y.; Wei, F.; Zheng, H.; Zhang, Y.; Li, F.; Chen, W. *PLoS ONE* **2015**, *10*, e0130683. DOI: 10.1371/journal.Pone.0130683.
17. Sun, Y.; Zheng, H.; Xiong, Z.; Wang, Y.; Tang, X.; Chen, W.; Ding, Y. *Desalin. Water Treat.* **2015**, *56*, 894.
18. Kahveci, M. U.; Beyazkilic, Z.; Yagci, Y. *J. Polym. Sci.: Part A: Polym. Chem.* **2010**, *48*, 4989.
19. Seabrook, S. A.; Gilbert, R. G. *Polymer* **2007**, *48*, 4733.
20. Zhang, J.; Bo, J.; Tan, G.; Zhai, L.; Fang, S.; Ma, Y. *Can. J. Chem. Eng.* **2015**, *93*, 1288.
21. Peng, X.; Peng, X.; Shen, J. *J. Appl. Polym. Sci.* **2007**, *103*, 3278.
22. Zhu, G.; Zheng, H.; Chen, W.; Fan, W.; Zhang, P.; Tshukudu, T. *Desalination* **2012**, *285*, 315.
23. Pal, S.; Sen, G.; Ghosh, S.; Singh, R. P. *Carbohydr. Polym.* **2012**, *87*, 336.
24. Akkaya, R. *Chem. Eng. J.* **2012**, *200-202*, 186.
25. Lin, C.; Chang, Y.; Gupta, J. P.; Shu, C. *Process Saf. Environ.* **2010**, *88*, 413.
26. Yang, Z.; Gao, B.; Li, C.; Yue, Q.; Liu, B. *Chem. Eng. J.* **2010**, *161*, 27.
27. Katsikas, L.; Popovic, I. G. *J. Phys. Chem. B* **2003**, *107*, 7522.
28. Abdollahi, Z.; Frounchi, M.; Dadbin, S. *J. Ind. Eng. Chem.* **2011**, *17*, 580.
29. Sawalha, O.; Scholz, M. *Ind. Eng. Chem. Res.* **2012**, *51*, 2782.
30. Wang, J.; Yuan, S.; Wang, Y.; Yu, H. *Water Res.* **2013**, *47*, 2643.
31. Verrelli, D. I.; Dixon, D. R.; Scales, P. J. *Colloids Surf. A* **2009**, *348*, 14.
32. Zhang, W.; Yang, P.; Yang, X.; Chen, Z.; Wang, D. *Bioresour. Technol.* **2015**, *181*, 247.
33. Zhao, Y. Q. *Chem. Eng. J.* **2003**, *92*, 227.
34. Neyens, E.; Baeyens, J. *J. Hazard. Mater.* **2003**, *B98*, 51.
35. Qi, Y.; Thapa, K. B.; Hoadley, A. F. A. *Chem. Eng. J.* **2011**, *171*, 373.
36. Zhang, W.; Yang, P.; Xiao, P.; Xu, S.; Liu, Y.; Liu, F.; Wang, D. *Colloids Surf. A* **2015**, *467*, 124.
37. Chakraborti, R.; Atkinson, J.; Vanbenschoten, J. *Environ. Sci. Technol.* **2000**, *34*, 3969.
38. Zheng, H.; Ma, J.; Zhu, C.; Zhang, Z.; Liu, L.; Sun, Y.; Tang, X. *Sep. Purif. Technol.* **2014**, *123*, 35.
39. Dong, Y.; Wang, Y.; Feng, J. *Water Res.* **2011**, *45*, 3871.